

# Mutant mitochondrial helicase Twinkle causes multiple mtDNA deletions and a late-onset mitochondrial disease in mice

Henna Tyynismaa\*, Katja Peltola Mjosund\*, Sjoerd Wanrooij†, Ilse Lappalainen\*, Emil Ylikallio\*, Anu Jalanko‡, Johannes N. Spelbrink†, Anders Paetau§, and Anu Suomalainen\*<sup>¶</sup>

\*Department of Neurology and Programme of Neurosciences, University of Helsinki, 00290, Helsinki, Finland; †Institute of Medical Technology and Tampere University Hospital, 33014, Tampere, Finland; ‡Department of Molecular Medicine, National Public Health Institute, 00290, Helsinki, Finland; and §Department of Pathology, Helsinki University Central Hospital and Haartman Institute, University of Helsinki, 00290, Helsinki, Finland

Edited by Giuseppe Attardi, California Institute of Technology, Pasadena, CA, and approved October 12, 2005 (received for review July 1, 2005)

**Defects of mitochondrial DNA (mtDNA) maintenance have recently been associated with inherited neurodegenerative and muscle diseases and the aging process. Twinkle is a nuclear-encoded mtDNA helicase, dominant mutations of which cause adult-onset progressive external ophthalmoplegia (PEO) with multiple mtDNA deletions. We have generated transgenic mice expressing mouse Twinkle with PEO patient mutations. Multiple mtDNA deletions accumulate in the tissues of these mice, resulting in progressive respiratory dysfunction and chronic late-onset mitochondrial disease starting at 1 year of age. The muscles of the mice faithfully replicate all of the key histological, genetic, and biochemical features of PEO patients. Furthermore, the mice have progressive deficiency of cytochrome c oxidase in distinct neuronal populations. These “deletor” mice do not, however, show premature aging, indicating that subtle accumulation of mtDNA deletions and progressive respiratory chain dysfunction are not sufficient to accelerate aging. This model is a valuable tool for therapy development and testing for adult-onset mitochondrial disorders.**

mouse model | progressive external ophthalmoplegia | mitochondrial DNA replication

**D**efects in nuclear-encoded proteins essential for mitochondrial DNA (mtDNA) maintenance have recently been shown to be important causes of mitochondrial disease. This disease group is characterized by progressive loss of mtDNA and/or somatic accumulation of multiple mtDNA deletions (1, 2). Defects of the mitochondrial replicative DNA polymerase  $\gamma$  (POLG) lead to a wide spectrum of neurological diseases, such as progressive external ophthalmoplegia (PEO), Alpers syndrome, parkinsonism and spinocerebellar ataxia (3–6). Furthermore, knock-in mice lacking the proofreading activity of POLG accumulated high amounts of mtDNA mutations and developed symptoms associated with advanced aging, supporting the role of mtDNA mutations also in normal aging (7).

We reported dominant mutations of the mitochondrial replicative helicase Twinkle in PEO with multiple mtDNA deletions (8). The disease manifested as myopathy, often affecting the extraocular, limb, and facial muscles, sometimes accompanied by major depression (9, 10). *In vitro*, Twinkle has been shown to form a minimal mtDNA replisome together with the mitochondrial single-stranded DNA-binding protein and POLG (11). We have recently demonstrated that Twinkle is essential for mtDNA maintenance because human cells devoid of Twinkle rapidly lost their mtDNA, and Twinkle has an active role in mtDNA copy number control *in vivo* (12). Twinkle bears homology to the bacteriophage T7 gp4 hexameric primase-helicase (8). PEO mutations are predicted to localize at or near the putative regions that link the subunits to the hexameric ring. Because the dNTP binding by the T7-type helicases occurs at the subunit interface, correct subunit interaction is essential for helicase activity (13, 14). Dominant mutations in Twinkle could therefore

both enhance dNTP breakdown and affect the processivity of mtDNA replication (8).

No effective treatment for mtDNA disease is available, and development of therapeutic strategies has been hindered by the lack of disease models that allow intervention and follow-up. Mouse models with mitochondrial dysfunction have been generated (15–18), but their severe disease course resembled that of childhood diseases and no models for chronic late-onset disease have been available. We examined the consequences of dominant Twinkle-PEO mutations in transgenic mice. These mice carrying human patient mutations have gradual worsening of the respiratory chain function due to accumulation of mtDNA deletions but show no signs of premature aging. They represent a previously uncharacterized mouse model for an adult-onset progressive mitochondrial disease.

## Materials and Methods

**Generation of Transgenic Twinkle Mice.** This work was approved by the National Public Health Institute animal care committee, and all experiments were done in accordance with good practice of handling laboratory animals.

We designed targeting constructs to carry the substitution of threonine for alanine at the amino acid 360 of mouse Twinkle protein (NP\_722491) (A360T, Twinkle<sup>AT</sup> mice hereafter), or an in-frame duplication of amino acids 353–365 (dup353–365, Twinkle<sup>dup</sup>). The production of wild-type Twinkle overexpressor mice (Twinkle<sup>WT+</sup>), serving as controls for possible quantitative effects of Twinkle expression, has been described in ref. 12. The mouse Twinkle cDNA and intron 4 was cloned into pHBApr-1-neo as described in ref. 12. The inclusion of the fourth intron allowed the expression of full-length Twinkle as well as its alternative splice variant Twinky. The p.A360T amino acid change corresponding to human p.A359T missense mutation was introduced with site-directed mutagenesis. To produce the dup353–365 mutation, a silent point mutation 1077C→G was introduced to form the restriction site Pfl23II, which was used to insert the 39-bp duplicated sequence with oligonucleotides. The primer sequences used are available upon request. The final DNA constructs were linearized with BglII and NdeI and used in pronuclear microinjection of FVB/N mouse fertilized oocytes. Genotyping of the mice and the transgene expression level determination were done as described in ref. 12.

**Morphologic Analysis.** Tissue samples were frozen in isopentane/liquid nitrogen. Cryostat sections from various tissue samples

Conflict of interest statement: No conflicts declared.

This paper was submitted directly (Track II) to the PNAS office.

Abbreviations: COX, cytochrome c oxidase; PEO, progressive external ophthalmoplegia; POLG, polymerase  $\gamma$ ; SDH, succinate dehydrogenase.

<sup>¶</sup>To whom correspondence should be addressed. E-mail: anu.wartiovaara@helsinki.fi.

© 2005 by The National Academy of Sciences of the USA



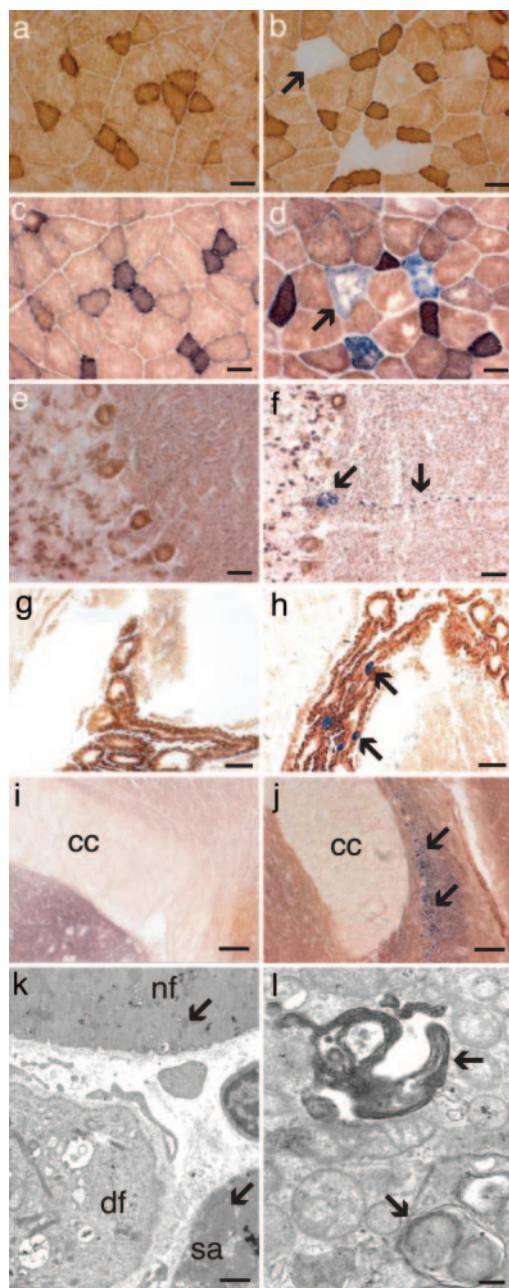


**Fig. 2.** Cytochrome c oxidase activity of muscle and brain and the skeletal muscle ultrastructure. Double staining for COX/SDH activities of the quadriceps femoris of 12-month-old control (a) and Twinkle<sup>dup</sup> mouse (b), the quadriceps femoris of 18-month-old control (c) and Twinkle<sup>dup</sup> (d) mouse, cerebellum of 18-month-old control (e) and Twinkle<sup>dup</sup> (f) mouse, choroid plexus of 18-month-old control (g) and Twinkle<sup>dup</sup> (h) mouse, and indusium griseum of 18-month-old control (i) and Twinkle<sup>dup</sup> (j) mouse (cc, corpus callosum). The arrows point to the affected cells of the transgenic mice. (k and l) Electron micrographs of ultrathin section of the quadriceps femoris of an 18-month-old Twinkle<sup>dup</sup> mouse. (k) Normal-sized mitochondrion is pointed out by the arrow in the normal fiber (nf) and an enlarged mitochondrion in the fiber with subsarcolemmal accumulation of mitochondria (sa). In the diseased fiber (df), muscle fibrils have been replaced by abnormal large mitochondria with inclusions, peripheral cristae, and vacuoles. (l) The autophagosomes with mitochondria found from the diseased fibers are shown by arrows. (Scale bars: 25  $\mu$ m, a–h; 100  $\mu$ m, i and j; 1  $\mu$ m, k; 200 nm, l.)

not show increased SDH activity (SDH<sup>+</sup>), indicating respiratory chain dysfunction without mitochondrial proliferation (Fig. 2b). Eighteen-month-old Twinkle<sup>dup</sup> mice exhibited both COX<sup>-</sup> and

COX<sup>-</sup>SDH<sup>+</sup> fibers, suggesting that COX-deficiency preceded mitochondrial proliferation (Fig. 2d). The percentage of COX<sup>-</sup> fibers increased gradually with age: average percentage at the age of 18–24 months was  $11.8 \pm 4.4\%$ , whereas it was  $0.03 \pm 0.01\%$  in the age-matched controls (mean  $\pm$  SD,  $P = 0.0008$ ). All three F<sub>1</sub> Twinkle<sup>dup</sup> mouse lines (C, D, and F) presented similar levels of COX<sup>-</sup> fibers. Twinkle<sup>AT</sup> mice presented a mild muscle phenotype because only a few COX<sup>-</sup> fibers were found. As Twinkle<sup>WT+</sup> mice or the nontransgenic littermates had virtually no COX<sup>-</sup> fibers even at the age of 22 months (Fig. 2a and c), COX<sup>-</sup> fibers were not a result of the normal aging process or overexpression of the mitochondrial protein *per se*, but a consequence of the transgene.

In electron microscopy of the Twinkle<sup>dup</sup> mouse muscle, several fibers had increased the number and size of mitochondria (Fig. 2k). In mildly affected fibers, the mitochondria were enlarged, and their number had increased in the subsarcolemmal region, but they still had recognizable cristae structures. In the severely affected fibers, however, the myofibrillar structure had been replaced by large mitochondria with concentric cristae, resembling onion-like structures, and electron-dense inclusions. These changes were identical to those in the muscle of PEO patients with Twinkle defects, with the exception that typical paracrystalline inclusions were not identified. Mitochondria were seen frequently within autophagosomes, indicating mitochondrial degradation (Fig. 2l).

The heart muscle sections of aging mutant and control mice had roughly equal levels of COX<sup>-</sup>SDH<sup>+</sup> fibers, similar to what has previously been reported for aging mice, indicating that our transgene did not substantially affect the heart muscle.

Biochemical analysis of the respiratory chain enzymes of a 20-month-old Twinkle<sup>dup</sup> F<sub>2</sub> mouse muscle, with the highest percentage of COX<sup>-</sup> fibers, showed moderately lowered COX activity and COX-dependent oxygen consumption with ascorbate as the substrate (50% and 64% of controls' mean, respectively, correlated against the nuclear-encoded complex II) (see supporting information, which is published on the PNAS web site). In many of the 20-month-old Twinkle<sup>dup</sup> F<sub>1</sub> mice, however, no significant reduction in the activities of the respiratory chain enzymes or oxygen consumption was detected, suggesting that the COX deficiency of individual muscle fibers was local and did not impair the total respiration capacity of the muscle.

**Deficiency of COX in Distinct Neuronal Populations.** Frozen brain sections of 18-month-old Twinkle<sup>dup</sup> mice showed that  $\approx 1\%$  of Purkinje cells in the cerebellum were COX<sup>-</sup>SDH<sup>+</sup> in both C and F lines, with COX deficiency and mitochondrial proliferation in the neuronal soma and dendrite (Fig. 2f). Other cerebellar cells had normal COX activity. In the cerebrum, large pyramidal neurons in the hippocampal CA2 region were mostly COX<sup>-</sup>SDH<sup>+</sup>, as well as neurons of indusium griseum, the region from which hippocampal cells developmentally derive (Fig. 2j). A few COX<sup>-</sup>SDH<sup>+</sup> neurons were also identified from the olfactory bulbs, substantia nigra, and the hypothalamus (data not shown). Many of the metabolically active and mitochondria-rich epithelial secretory cells of the choroid plexus were also COX<sup>-</sup>SDH<sup>+</sup> (Fig. 2h). No COX<sup>-</sup>SDH<sup>+</sup> neurons or other brain cells were found from age-matched control littermates or Twinkle<sup>WT+</sup> mice (Fig. 2e, g, and i). The COX<sup>-</sup> regions could reflect either  $\beta$ -actin expression pattern or sensitivity of the affected cells to mitochondrial dysfunction. The regions with the highest endogenous  $\beta$ -actin expression in mouse brain are the olfactory bulbs, motor cortex, and choroid plexus (22), of which the first and third showed evident COX<sup>-</sup> deficiency in our mice, whereas no COX<sup>-</sup> neurons were identified in the pyramidal neurons of the motor cortex.

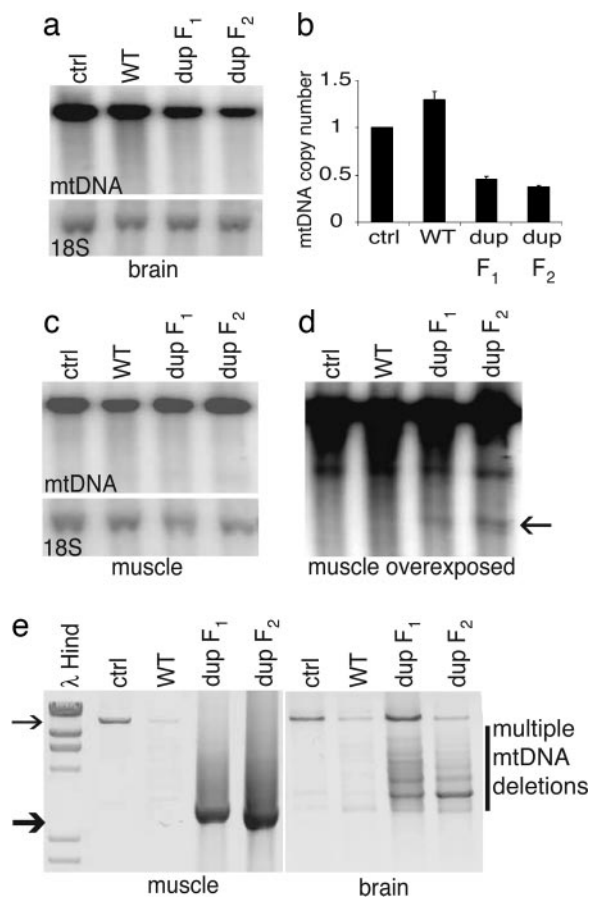


**Fig. 3.** Mitochondrial DNA analysis and copy number determination. (a and c) Southern blots of muscle and brain DNA of 22-month-old control, Twinkle<sup>WT</sup> mice, and Twinkle<sup>dup</sup> F<sub>1</sub> mouse and an 18-month-old Twinkle<sup>dup</sup> F<sub>2</sub> mice probed with mtDNA, and nuclear 18S rRNA gene. (b) Quantitation of brain mtDNA copy number of the mice against the nuclear 18S rRNA gene. (d) Overexposed Southern blot of muscle DNA shown in c. The 3-kb band found from Twinkle<sup>dup</sup> mice is pointed by the arrow. (e) Long PCR of muscle and brain DNA of the same mice. The full-length mtDNA is indicated by the thin arrow and the most prevalent deletion molecule size of muscle mtDNA ( $\approx$ 3 kb) by the thick arrow.

**Mutant Mice Accumulate Mitochondrial DNA Deletions.** We searched for multiple mtDNA deletions in our Twinkle<sup>dup</sup> and control mice by long PCR and by Southern hybridization analysis, because these types of mutations accumulate in Twinkle-PEO patients. Amplification of brain mtDNA of Twinkle<sup>dup</sup> mice resulted in multiple products, corresponding to full-size mtDNA and molecules with deletions of multiple sizes (Fig. 3e). Only the 16-kb product was amplifiable from the control brain. The similar deletion pattern of the brain mtDNA in different mice indicated deletion hotspots. However, from the muscle, only a single product of  $\approx$ 3 kb was readily amplified, whereas the 16-kb product from the wild-type mtDNA amplified from all of the control samples (Fig. 3e). DNA sequence analysis revealed that this 3-kb product represented multiple different deletion molecules, which all had their 5' breakpoints between 2707–3020 and 3' breakpoints between 15376–15441 (supporting information). Only 12S rRNA, 16S rRNA, and the noncoding region of mtDNA remained in these molecules (Fig. 4a). The deletions could not be seen on Southern blots (Fig. 3a and c), except for the 3-kb mutant population in the muscle, seen in the samples of Twinkle<sup>dup</sup> F<sub>1</sub> and F<sub>2</sub> mice upon overexposure of autoradiography, estimated to constitute  $\approx$ 5% of total mtDNA in the muscle (Fig. 3d). We used laser-capture microdissection to obtain DNA

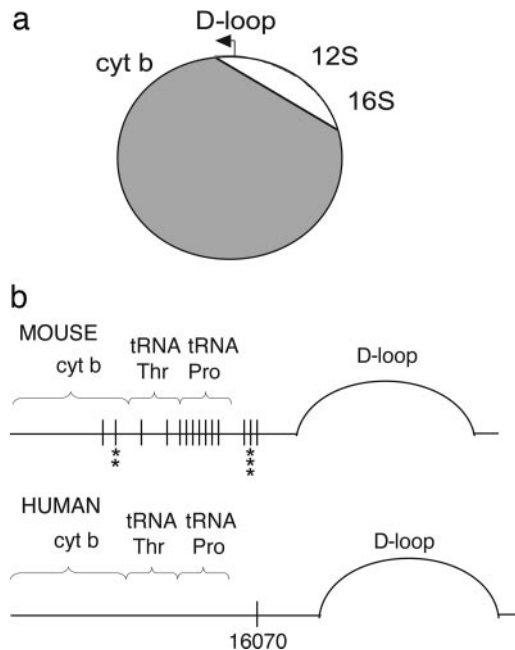


**Fig. 4.** mtDNA deletions of the muscle and brain of the Twinkle<sup>dup</sup> mouse, determined by long PCR, cloning, and DNA sequencing. (a) Schematic diagram of mouse mtDNA showing the deleted segment in gray (see supporting information for details). Only the D-loop, 12S rRNA, and 16S rRNA were commonly spared. (b) Schematic presentation of the mouse and human mtDNA region harboring the 5' deletion breakpoints. Black vertical lines show the 5' deletion breakpoints identified in this study, and the asterisks below indicate how often the same 5' breakpoint was found from dissimilar deletion molecules. The common 5' deletion breakpoint of human multiple mtDNA deletions (16070) is indicated.

from single muscle fibers and were able to correlate the deletion molecules with some COX<sup>-</sup> fibers and not any of the COX<sup>+</sup> fibers by single-fiber PCR (data not shown). The heart DNA of aging mice, mutated or control, contained multiple mtDNA deletions both by long PCR and overexposed Southern blot, but they were not in excess in the mutant mouse heart (data not shown). Quantification of mtDNA copy number against the nuclear 18S rRNA gene in Twinkle<sup>dup</sup> mouse tissues revealed a clear mtDNA depletion in the brain (46% of control value in dup F<sub>1</sub> mice and 37% in dup F<sub>2</sub> mice,  $P < 0.0001$  for both; Fig. 3b). In the muscle and the heart of the Twinkle<sup>dup</sup> mice, mtDNA levels were similar to those of the nontransgenic littermates.

Our 18-month-old Twinkle<sup>dup</sup> mice did not have an increased somatic mtDNA point mutation load in their muscle samples: Only 0.45 mutations per 10 kb in the cytochrome *b* region and 0.25 mutations in the control region were present, when  $>33$  kb of cloned mtDNA sequence was analyzed per mouse.

**The Physical Performance of the Mice Is Not Compromised.** Because of the marked histological changes in the muscle, we studied the muscle strength and performance of our mice. The rotating bar, Rotarod, performance reflects the ability to sustain complex coordinated movements; the test of Twinkle<sup>dup</sup> and Twinkle<sup>AT</sup> mice showed no statistical significant difference compared to the littermates (supporting information). Likewise, the maximal grip strength was not affected by the muscle changes and was similar to the control littermates. The distance run on voluntary running-wheel exercise has been shown to reflect the endurance capacity. We found no signs of significant muscle weakness or impairment of exercise capacity in Twinkle<sup>dup</sup> or Twinkle<sup>AT</sup> mice, but the daily running duration and distance of the transgenic mice was higher compared to controls ( $P = 0.05$ ). The

distance per day for each week (mean  $\pm$  SD) was  $1.3 \pm 0.5$  km in controls,  $2.6 \pm 0.6$  km in mice harboring the Twinkle<sup>AT</sup> mutation, and  $3.7 \pm 0.7$  km in the Twinkle<sup>dup</sup> mice (supporting information).

## Discussion

We report here a mouse model for an adult-onset mitochondrial disease. Our transgenic mice, expressing the mitochondrial Twinkle helicase with dominant PEO mutations, replicated faithfully the key histological and molecular findings of the human PEO disease. This model developed a morphologically clear mitochondrial myopathy but affected the well being of the mouse only mildly, thus offering great promise for evaluation of therapeutic strategies.

The Twinkle mutations expressed in the mice corresponded to two PEO patient mutations, dup352–364 and A359T. The in-frame duplication is the structurally most severe mutation so far described in Twinkle. The A359T mutation was chosen, because in bacteriophage T7, the analogous mutation A257T was a gain-of-function mutation, resulting in enhanced dTTPase activity of the helicase (23). The patients with dup352–364 presented with autosomal dominant PEO, generalized muscle weakness, avoidant personality traits, and major depression with the age of onset between 20 to 51 years (8, 9). The missense mutation A359T in human patients caused late-onset PEO at  $\approx$ 50 years with moderate myopathy and no CNS involvement (M. Zeviani, personal communication). Our Twinkle<sup>dup</sup> mice developed the first histological signs of mitochondrial myopathy at the age of 12 months, mimicking the relative age of onset of human disease when related to the expected lifespan. The myopathy of the mice progressed, as judged by the growing severity of the morphological changes. The amount of COX<sup>-</sup> muscle fibers in PEO patients with dup352–364 was 2–11% (9) and in Twinkle<sup>dup</sup> mice was  $\approx$ 12%. The three independent Twinkle<sup>dup</sup> transgenic lines developed the same muscle phenotype showing that the muscle changes were caused by the mutant Twinkle and not by the transgene insertion site. The Twinkle<sup>AT</sup> mice with the homologous mutation presented a slow progression of COX deficiency compared to the Twinkle<sup>dup</sup> mice. The overall mouse muscle phenotype closely mimics the findings in the PEO patients.

A hallmark of the PEO disease is the accumulation of multiple large mtDNA deletions in the patients' postmitotic tissues, the mutant mtDNA reaching up to 60% of total mtDNA in some brain regions and 40% in the skeletal muscle (1, 24). We observed accumulation of similar deletions in the corresponding mouse tissues. The number of deletion molecules increased with age, along with the progressive respiratory chain dysfunction, judged by the increase of the COX-deficient fibers. However, the amount of deleted mtDNA in the mice was quite low, resembling the findings in juvenile PEO patients with dup352–364 mutation (9) and in patients with POLG-related ataxias (4). The low mutant mtDNA amount may reflect the short lifespan of mice: in humans mtDNA deletions became visible in Southern blot at only  $\approx$ 20 years of age, whereas our mice were maximally  $\approx$ 2 years when killed. Interestingly, the low number of mutant mtDNA did not reflect the quantity of COX-deficient muscle fibers, because the number of abnormal fibers was similar in PEO patients and our mice. Our mice had the somatic point mutation load and total mtDNA copy number similar to controls in their muscle and, therefore, these factors did not exacerbate COX deficiency. The COX deficiency seemed to clearly precede the mitochondrial accumulation, because 1-year-old mice had some completely COX<sup>-</sup> fibers, but SDH<sup>+</sup> fibers were first observed in 18-month-old mice.

The muscle atrophy and mitochondrial dysfunction caused surprisingly little functional consequences in our mice. Biochemical analysis showed mildly decreased or low normal activities of the respiratory chain enzyme complexes I, III, and IV. These

complexes contain mtDNA-encoded subunits, and the finding strongly supports the causal relationship of mtDNA defects and respiratory chain deficiency. Similar activities are typical for PEO patients with dup352–364 (9), reflecting the low proportion of affected fibers in the muscle homogenate. The physical performance, exercise capacity and muscle strength, of our mice was good. Actually, the mutant mice seemed to exercise voluntarily slightly more than their wild-type littermates. It is tempting to speculate that the increased urge to run would be a consequence of the transgene: a result of direct brain involvement or spontaneous behavior to compensate for the muscle atrophy. However, these conclusions require further studies with a large number of mice with different genetic background. We show, however, that mouse muscle tolerates a considerable number of dysfunctional fibers until its function becomes compromised. This phenotype agrees well with the findings in Twinkle<sup>dup</sup> patients, who often have considerable subjective exercise intolerance but mild objective muscle weakness (25).

To examine the deletion mechanisms, we characterized in detail the mtDNA deletion breakpoints in the brain and muscle of our mice. The Twinkle<sup>dup</sup> mouse muscle harbored mutant mtDNA, the majority of which carried a  $\approx$ 13-kb nonclonal mtDNA deletion. The products all consisted only of rRNA genes and the D-loop region but had individual 5' and 3' breakpoint sequences at close-by sites. These breakpoints either contained no or short direct repeats of 4–5 bp, consistent with class II deletions. These 3-kb "minimal mtDNA molecules" closely resembled the 3.75-kb "common sublimons" previously found in the control human heart (26). The brain mtDNA also resulted in a range of amplification products from full-length to  $\approx$ 3 kb in size. This deletion pattern closely resembled the findings in human patients (24). Upon breakpoint analysis, we identified similar deletion hotspots in the brain as in the muscle, suggesting that these sites form a major deletion hotspot in Twinkle mice. Most importantly, the 3' deletion breakpoints, bp 15180–15441 of mouse mtDNA, overlapped with the human base pair 16070, a previously described breakpoint hotspot of PEO-Twinkle patients (27) and the common sublimon (26). Furthermore, a recent study targeted PstI restriction enzyme to the mouse skeletal muscle mitochondria, resulting in continuous generation of double-strand breaks. These mice had 3' PstI-independent deletion breakpoints at bp 15368–15439 (28), overlapping with our breakpoints. The hotspot region in human and mouse mtDNA is located between tRNA<sup>Phe</sup> and the D-loop and contains the most highly divergent primary sequence of mtDNA (29). It seems evident that the general mechanism causing multiple deletions with breakpoints at the specific site is not due to the primary sequence itself but its secondary structure or functional location. The PstI mice strongly suggested that double-strand breaks mediate the formation of class II mtDNA deletions in mammals (28). The intriguing hypothesis arising from the present and previous data are that the primary consequence of Twinkle<sup>dup</sup> defect was generation of double-strand breaks, as we have suggested based on deletion breakpoint analysis of PEO-Twinkle patients (27). Furthermore, we suggest a specific conserved role for the hotspot region in double-strand break repair or as a recombination site for free 5' ends of the double-strand breaks.

POLG and Twinkle defects have recently been found to underlie a wide phenotype range expanding to neurodegenerative diseases (4, 5). Therefore, we carefully looked for CNS involvement in two different Twinkle<sup>dup</sup> mouse lines. We identified populations of large neurons that were COX<sup>-</sup>SDH<sup>+</sup> in both lines: cerebellar Purkinje cells, hippocampal CA2 pyramidal neurons, and those of indusium griseum. The COX deficiency in these neurons may result from mtDNA depletion or accumulation of deleted mtDNA in selected cells. COX-deficient Purkinje cells have not been previously reported in

mice or in humans. Loss of Purkinje cells was noted in an autopsy of PEO patient with dup352–364 mutation and in mtDNA maintenance defects, such as mitochondrial spinocerebellar ataxia and Alpers syndrome (4, 6, 24). Notably, the COX<sup>-</sup>SDH<sup>+</sup> hippocampal neurons in our mice resembled closely those reported in aged humans and in Alzheimer patients (30, 31). In our mice, the neuronal COX deficiency did not directly follow the expression pattern of mouse  $\beta$ -actin, and the deficiency may manifest in those neuronal populations that are most susceptible to defects in mtDNA maintenance and mitochondrial dysfunction. Thus, our mouse model provides a promising tool to understand neuronal cell type-specific mtDNA maintenance.

MtDNA mutations have recently been linked to premature aging because the mice with proofreading-deficient POLG were found to have large numbers of somatic mtDNA point mutations already at the age of two months and to present phenotypes associated with aging in mammals (7). The “mutator mice” were reported to also have deleted, linear mtDNA, the amount of which did not increase over time. Twinkle is the partner of POLG in replication, and it was of interest to notice that our deleter mice did not age prematurely, although they accumulate mtDNA deletions, leading to progressive respiratory chain deficiency. Our data suggest that premature aging might require extensive mtDNA mutagenesis, or alternatively, the phenotype of the mutator mice is due to a specific function of POLG protein not associated with mtDNA mutagenesis.

The Twinkle<sup>dnp</sup> mice are mtDNA disease models that replicate the manifestations of a specific patient mutation. Previous mouse models for mitochondrial respiratory dysfunction include gene knockouts of essential proteins for mtDNA maintenance: inactivation of adenine-nucleotide translocator-1 resulted in myopathy and cardiac hypertrophy at 4–6 months of age (15).

Tissue-specific knockouts of Tfam elucidated the consequences of the loss of mitochondrial transcripts and severe respiratory chain deficiency in specific cell types (18). The  $\Delta$ mtDNA mice had high levels of a single mtDNA deletion in most tissues already at birth (17), resulting in respiratory chain deficiency in heart, skeletal muscle, and kidney and making it a good model for an early onset multisystem mitochondrial disease. The  $\Delta$ mtDNA mice died at 6 months of age due to renal failure. Mice expressing PstI in mitochondria developed mitochondrial myopathy at 7 months of age but could not reproduce (28). In contrast to all previous models, the Twinkle<sup>dnp</sup> mice specifically model a late-onset progressive mitochondrial disease without compromising lifespan or reproduction.

Therapy trials for mitochondrial disorders are exceptionally challenging, because large homogeneous patient materials allowing double-blind test setups are not available even in large centers. Our transgenic Twinkle<sup>dnp</sup> mouse model enables studies of long- and short-term effects of exercise or different therapeutic ideas in a double-blinded setting, with genetically homogeneous and large study material. It enables follow-up of presymptomatic disease progression and intervention, as well as tests directed to reveal the pathogenesis of a late-onset disease. These deleter mice are an ideal tool to study mtDNA disease.

We thank the staff from the animal units of National Public Health Institute and Haartman Institute for skillful assistance. This work was supported by Helsinki Biomedical Graduate School (H.T.); Academy of Finland Centre of Excellence program (A.S. and J.N.S.); Sigrid Juselius Foundation and Helsinki University research funds (to A.S.); and the Medical Research Fund of Tampere University Hospital and the European Community's Sixth Framework Program for Research Priority 1 “Life Sciences, Genomics, and Biotechnology for Health” Contract LSHM-CT-2004-503116 (to J.N.S.).

- Zeviani, M., Servidei, S., Gellera, C., Bertini, E., DiMauro, S. & DiDonato, S. (1989) *Nature* **339**, 309–311.
- Moraes, C. T., Shanske, S., Tritschler, H. J., Aprille, J. R., Andreetta, F., Bonilla, E., Schon, E. A. & DiMauro, S. (1991) *Am. J. Hum. Genet.* **48**, 492–501.
- Van Goethem, G., Dermaut, B., Lofgren, A., Martin, J. J. & Van Broeckhoven, C. (2001) *Nat. Genet.* **28**, 211–212.
- Van Goethem, G., Luoma, P., Rantamaki, M., Al Memar, A., Kaakkola, S., Hackman, P., Krahe, R., Lofgren, A., Martin, J. J., De Jonghe, P., et al. (2004) *Neurology* **63**, 1251–1257.
- Luoma, P., Melberg, A., Rinne, J. O., Kaukonen, J. A., Nupponen, N. N., Chalmers, R. M., Oldfors, A., Rautakorpi, I., Peltonen, L., Majamaa, K. et al. (2004) *Lancet* **364**, 875–882.
- Naviaux, R. K. & Nguyen, K. V. (2004) *Ann. Neurol.* **55**, 706–712.
- Trifunovic, A., Wredenberg, A., Falkenberg, M., Spelbrink, J. N., Rovio, A. T., Bruder, C. E., Bohlooly, Y. M., Gidlof, S., Oldfors, A., Wibom, R. et al. (2004) *Nature* **429**, 417–423.
- Spelbrink, J. N., Li, F. Y., Tiranti, V., Nikali, K., Yuan, Q. P., Tariq, M., Wanrooij, S., Garrido, N., Comi, G., Morandi, L. et al. (2001) *Nat. Genet.* **28**, 223–231.
- Suomalainen, A., Majander, A., Wallin, M., Setala, K., Kontula, K., Leinonen, H., Salmi, T., Paetau, A., Haltia, M., Valanne, L. et al. (1997) *Neurology* **48**, 1244–1253.
- Lewis, S., Hutchison, W., Thyagarajan, D. & Dahl, H. H. (2002) *J. Neurol. Sci.* **201**, 39–44.
- Korhonen, J. A., Pham, X. H., Pellegrini, M. & Falkenberg, M. (2004) *EMBO J.* **23**, 2423–2429.
- Tyynismaa, H., Sembongi, H., Bokori-Brown, M., Granycome, C., Ashley, N., Poulton, J., Jalanko, A., Spelbrink, J. N., Holt, I. J. & Suomalainen, A. (2004) *Hum. Mol. Genet.* **13**, 3219–3227.
- Sawaya, M. R., Guo, S., Tabor, S., Richardson, C. C. & Ellenberger, T. (1999) *Cell* **99**, 167–177.
- Singleton, M. R., Sawaya, M. R., Ellenberger, T. & Wigley, D. B. (2000) *Cell* **101**, 589–600.
- Graham, B. H., Waymire, K. G., Cottrell, B., Trounce, I. A., MacGregor, G. R. & Wallace, D. C. (1997) *Nat. Genet.* **16**, 226–234.
- Huo, L. & Scarpulla, R. C. (2001) *Mol. Cell. Biol.* **21**, 644–654.
- Inoue, K., Nakada, K., Ogura, A., Isobe, K., Goto, Y., Nonaka, I. & Hayashi, J. I. (2000) *Nat. Genet.* **26**, 176–181.
- Larsson, N. G. & Rustin, P. (2001) *Trends Mol. Med.* **7**, 578–581.
- Spelbrink, J. N., Toivonen, J. M., Hakkaart, G. A., Kurkela, J. M., Cooper, H. M., Lehtinen, S. K., Lecrenier, N., Back, J. W., Speijer, D., Foury, F. et al. (2000) *J. Biol. Chem.* **275**, 24818–24828.
- Majander, A., Rapola, J., Sariola, H., Suomalainen, A., Pohjavuori, M. & Pihko, H. (1995) *J. Neurol. Sci.* **134**, 95–102.
- Allen, D. L., Harrison, B. C., Maass, A., Bell, M. L., Byrnes, W. C. & Leinwand, L. A. (2001) *J. Appl. Physiol.* **90**, 1900–1908.
- Zapala, M. A., Hovatta, I., Ellison, J. A., Wodicka, L., Del Rio, J. A., Tennant, R., Tynan, W., Broide, R. S., Helton, R., Stoveken, B. S., et al. (2005) *Proc. Natl. Acad. Sci. USA* **102**, 10357–10362.
- Washington, M. T., Rosenberg, A. H., Griffin, K., Studier, F. W. & Patel, S. S. (1996) *J. Biol. Chem.* **271**, 26825–26834.
- Suomalainen, A., Majander, A., Haltia, M., Somer, H., Lonnqvist, J., Savontaus, M. L. & Peltonen, L. (1992) *J. Clin. Invest.* **90**, 61–66.
- Lofberg, M., Lindholm, H., Naveri, H., Majander, A., Suomalainen, A., Paetau, A., Sovijarvi, A., Harkonen, M. & Somer, H. (2001) *Neuromuscul. Disord.* **11**, 370–375.
- Kajander, O. A., Rovio, A. T., Majamaa, K., Poulton, J., Spelbrink, J. N., Holt, I. J., Karhunen, P. J. & Jacobs, H. T. (2000) *Hum. Mol. Genet.* **9**, 2821–2835.
- Wanrooij, S., Luoma, P., van Goethem, G., van Broeckhoven, C., Suomalainen, A. & Spelbrink, J. N. (2004) *Nucleic Acids Res.* **32**, 3053–3064.
- Srivastava, S. & Moraes, C. T. (2005) *Hum. Mol. Genet.* **14**, 893–902.
- Walberg, M. W. & Clayton, D. A. (1981) *Nucleic Acids Res.* **9**, 5411–5421.
- Cottrell, D. A., Blakely, E. L., Johnson, M. A., Ince, P. G., Borthwick, G. M. & Turnbull, D. M. (2001) *Neurobiol. Aging* **22**, 265–272.
- Cottrell, D. A., Blakely, E. L., Johnson, M. A., Ince, P. G. & Turnbull, D. M. (2001) *Neurology* **57**, 260–264.